CASE STUDY OF CORE-STIFFENED WING VERSUS SKIN-STRINGER APPROACH FOR INTERMEDIATE-SIZE FLIGHT STRUCTURES

Jeffrey M. Perkins, Richard K. Dropek
Radius Engineering, Inc.
Salt Lake City, Utah

ABSTRACT

Advanced Air Mobility (AAM) companies aim to produce a new style of aircraft, with new materials at a pace and scale that has not yet been accomplished in the composites aerospace industry. Many material options and manufacturing processes exist for prospective manufacturers who are looking to optimize the performance and minimize the weight of composite structures. Vehicle weight, manufacturing efficiency, and FAA certification are a few of the top considerations for AAM designers.

This paper presents the results of an engineering study conducted to compare two different approaches for representative AAM vehicle primary structures. Equivalent core-stiffened and skin-stringer wing designs were developed for a typical mid-size (~12-meter) aircraft structure. The composite design, along with the tooling and equipment required for manufacturing, were evaluated for the wing skin and spar.

Equivalency comparisons were made for buckling, overall strength, structural deflections, and weight using typical loading scenarios. The composite study showed that the skin-stringer designs may have equivalent or improved performance when compared to the core-stiffened wing designs. The stringer and intercostal designs act as a gateway allowing for the closed mold Same Qualified Resin Transfer Molding (SQRTM) prepreg manufacturing approach to provide FAA certifiable structures with improved quality and repeatability. This may also accelerate FAA certification while simultaneously enabling a transition to out-of-autoclave (OOA) processing.

Keywords: AAM, Design, Out of Autoclave, OOA, Net-Shape, SQRTM, Wing Structure
Corresponding author: Jeffrey M. Perkins

1. INTRODUCTION

Advanced Air Mobility (AAM) companies and their potential manufacturing partners need to move rapidly to establish flight structure designs that achieve their goals for performance, manufacturing efficiency, and speed to market. Radius Engineering is a leader in the development and implementation of OOA Net-Shape advanced composites manufacturing technologies for flight critical structures and propulsion systems. This paper offers a comparative analysis of two approaches for the design and manufacturing of intermediate-size flight structures that are well suited for AAM vehicles: 1) Core stiffened structures vs. 2) "Skin-

Stringer" stiffened structures. The term "skin-stringer" is used here to represent skins or spars stiffened by upstanding blade structures such as ribs, intercostals, and stringers.

1.1 AAM Vehicle Characteristics

AAM vehicles are designed for a variety of urban and regional flight missions carrying passengers and cargo. The design concepts vary based on the missions they are intended to complete and the experiences of the design team developing them, but they can generally be categorized into three groups:

1. Lift & Cruise
2. Vectored Thrust / Tilt Rotor
3. Augmented Lift

Most of these vehicles have wingspans in the range of 9-17 meters (30-55 feet) and Maximum Take-off Weights (MTOW) in the range of 2,300 – 3,200 kg (5,000 – 7,000 lbs) [1][2]. For the purposes of this comparative analysis an intermediate-size Vectored Thrust / Tilt Rotor vehicle with a wingspan of approximately 12.2 m (40 ft) and an MTOW of 2,720 kg (6,000 lbs) has been considered with both design / manufacturing approaches. Figure 1 and Figure 2 show the range of typical vehicle designs being developed.

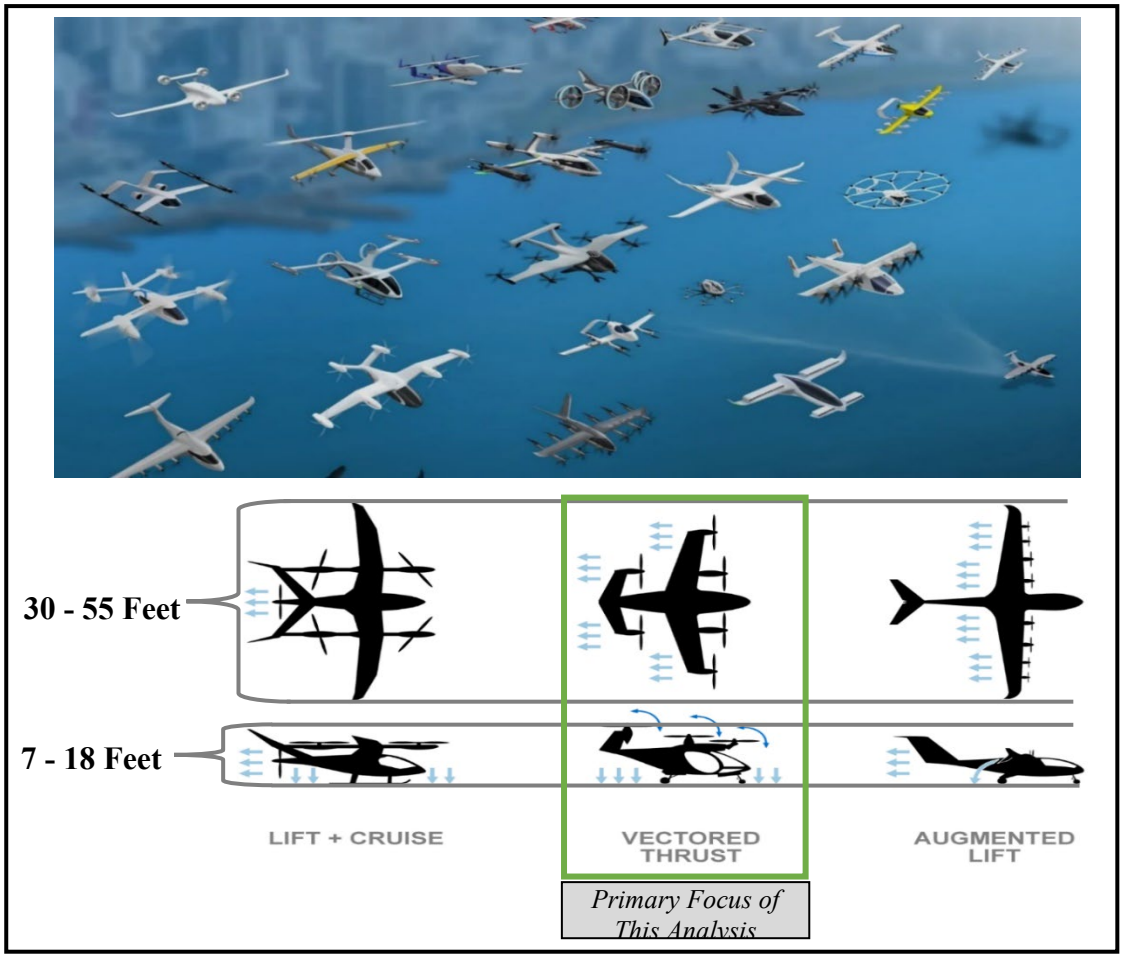

Figure 1: Many Vehicle Concepts - Similar Flight Structures [1]

	Tilt-Duct eVTOL	Tilt-Rotor eVTOL	eSTOL
MTOW (lb)	6000	6000	6000
Payload (lb)	**767**	**1116**	**1963**
Usable Range (nmi)	300	300	300
Fuel (lb)	438	553	539
Battery (lb)	710	433	226
Installed Motor Power (kW)	1,886	1,769	576
Turbine Power (kW)	216	266	260
Cruise L/D	14.8	10.3	10.5
$f_{batt,TO}$	0.87	0.75	0.62
Cruise Alt. (ft MSL)	5,000	5,000	10,000
		Primary Focus of This Analysis	

Figure 2: Predicted Characteristics of Various Vehicle Types [2]

1.2 Core Stiffened and Skin-Stringer Flight Structures

The flight structures analyzed in this study include a wing skin panel and a main wing spar, as these structures are broadly applicable to a variety of AAM vehicles. However, the same comparative analysis can be performed for a variety of structures to determine which approach is best suited for the function.

Core stiffened structures can also be described as sandwich panels, typically comprised of a bottom layer of pre-impregnated carbon fiber (prepreg), then a foam or honeycomb core, and a finally a top layer of carbon fiber prepreg. The panels are generally categorized as symmetrical or asymmetrical panels, where symmetrical panels are more suited for pressurized structures and asymmetrical panels are more optimized for mass reduction on non-pressurized structures subjected to low loads on light aircraft [4]. Symmetrical panels utilize an upper skin and a lower skin that are symmetrical about the core. Asymmetrical panels utilize a first skin, called the "Working Skin" that takes most of the membrane stresses and a second skin that is designed to the minimum allowed called the "Stabilizing Skin" [4]. For the purposes of this analysis an asymmetrical panel construction with prepreg and closed cell foam was considered, as seen in Figure 3.

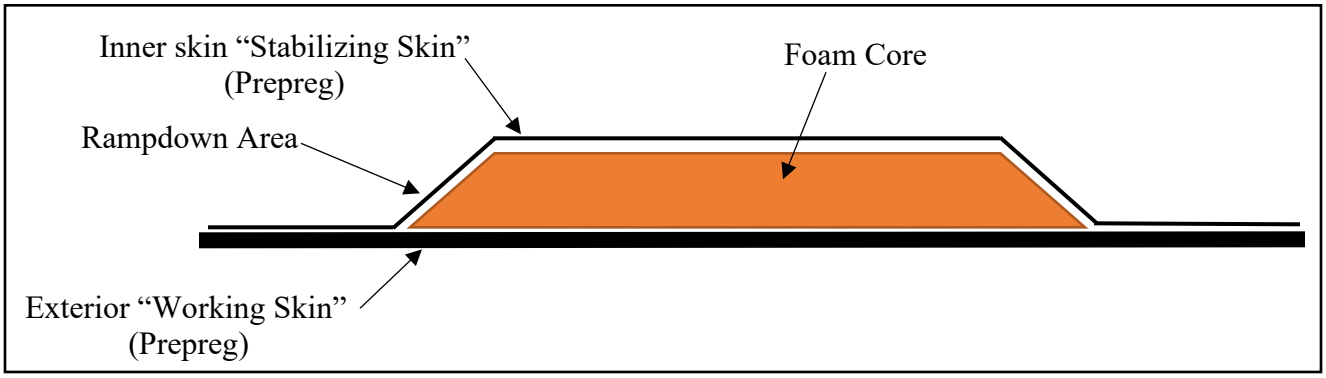

Figure 3: Basic Core Stiffened Panel Construction [4]

Skin-stringer stiffened structures can also be described as monolithic structures (without a core) and are comprised of carbon fiber prepreg with integrated (co-cured) stiffeners such as intercostals on a spar and stringers on a wing skin. Skin-stringer stiffened structures are produced with a variety of manual and automated layup methods and are compatible with out-of-autoclave (OOA), closed mold processes such as Same Qualified Resin Transfer Molding (SQRTM). These structures are also compatible with resin infusion processes such as Resin Transfer Molding (RTM), although RTM processing was not considered as part of this comparative analysis. Figure 4 shows the typical construction of skin-stringer designs utilizing a skin, L-flange preforms, and a radius filler ("noodle").

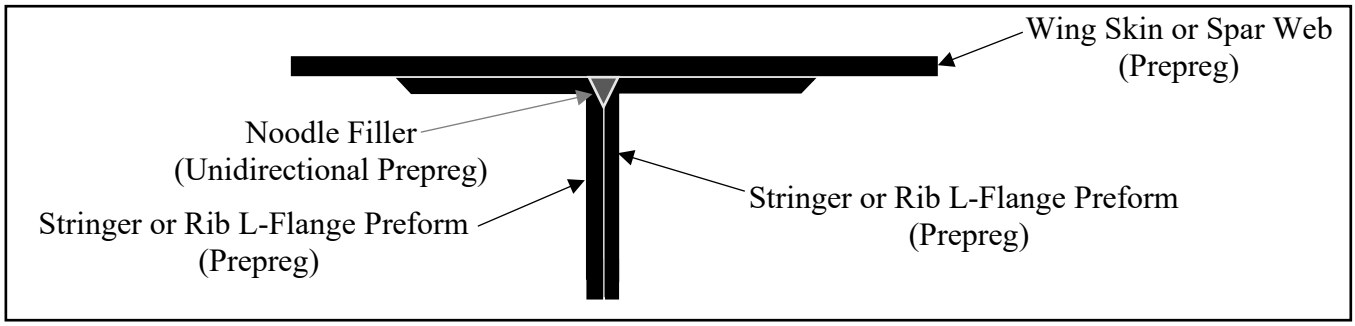

Figure 4: Rib or Stringer Stiffener Basic Construction

Figure 5 shows two example flight structures where the image on the left utilizes a core-stiffened design and the image on the right utilizes a skin-stringer design.

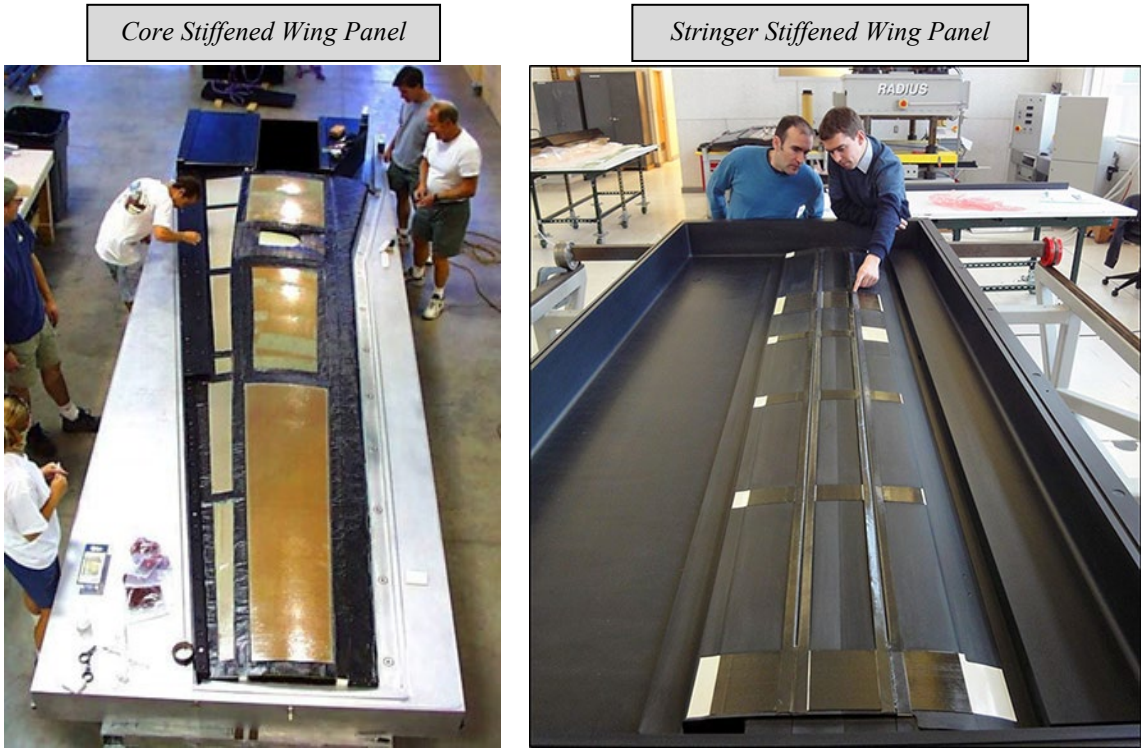

Figure 5: Core-Stiffened vs. Stringer Stiffened Wing Panels

1.3 Skin-Stringer design benefits

Skin-stringer designs for primary flight structures, such as wing skins and spars, can achieve higher performance with equivalent or reduced weights when compared to core-stiffened designs. A higher level of structural integration is possible with closed mold manufacturing processes [3], enabling further reductions in overall weight when the design concepts move beyond what is possible with core stiffened structures [5]. Higher fiber volume laminates with reduced void content may be attained due to laminate compaction pressures during cure (7-8 bar), not achievable with low density foam core materials.

The rib-stringer design concept also enables higher levels of automation in manufacturing and tighter process control with the SQRTM process [3]. The SQRTM process utilizes the "Same Qualified" prepregs with existing allowable databases to accelerate the FAA certification process, while also establishing a manufacturing process that is compatible with future fast-cure material systems that may be considered for future vehicle designs.

2. CASE STUDY DETAILS

Design and analysis results are presented here comparing core stiffened versus skin stringer stiffened designs. The two structures chosen for this study were a representative wing panel and a main wing spar. The finite element method was used to analyze the structures. Nastran was used as the solver while FEMAP was used as the pre- and post- processor. The composite laminate was modeled with Nastran CQUADR and CTRIAR shell elements with ply-by-ply layups defined with the PCOMP material property input. Nastran 3D solid CHEXA and CPENTA elements were used to model the core. Nastran CBAR beam elements were used to simulate pultruded UD tape noodles used at the junctions of formed stringers and ribs.

Laminate material used was a typical aerospace epoxy carbon fiber (Toray T800) woven prepreg of 190 gsm areal weight, for 125℃ cure. Foam core material modeled was a closed cell core of ~75 kg/m3, typically PVC, PMI or polyurethane.

2.1 Wing Skin Design Concepts

Figure 6 shows a representative straight wing geometry with approximately 12 m (40 ft) span that was conceptualized. A wing panel, situated between inboard and outboard ribs, a leading-edge spar, and a trailing edge stringer, was selected for analysis.

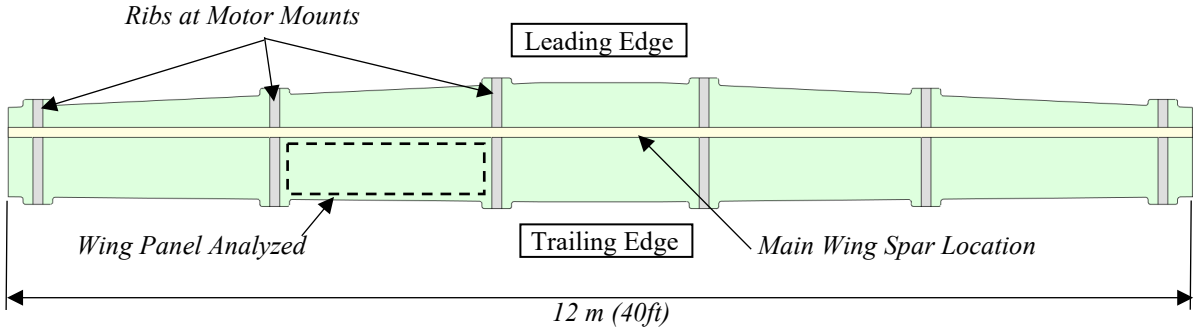

Figure 6: Representative Wing Geometry

The analysis was done comparing a core stiffened wing panel to a stringer and rib stiffened panel. The analyses were intended as a one-to-one comparison only and not intended to represent a final design. The two designs were situated at the same wing location and subjected to the same load states and boundary conditions. Figure 7 shows the basic shape of the wing panel segment.

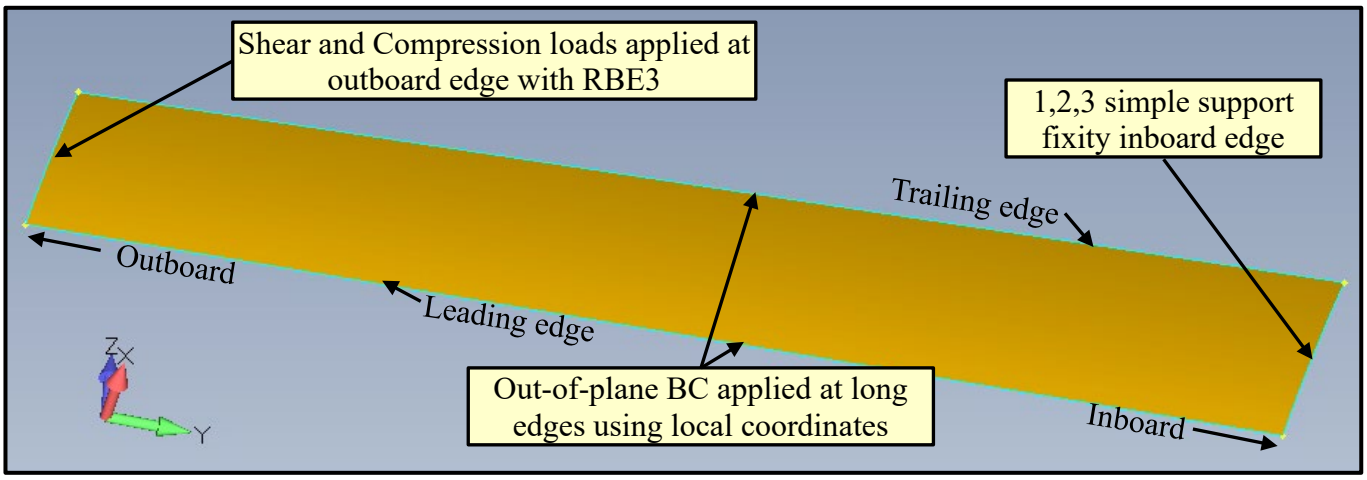

Figure 7: Basic wing panel and boundary condition description

Both designs were checked for buckling, deflection, and strength. The load states applied to the wing panel segments are listed in Table 1 and are typical of an aircraft of this size and MTOW. General boundary conditions used in analyses are described in Figure 7 and Table 2. The overall purpose of the boundary restraints was to allow full buckling wave forms to develop while simulating the restraining effects at the boundaries of ribs, wing spar, and trailing edge stringer. Because of the tapered and curved nature of the wing panel, local coordinates were established and used at the panel edges to correctly orient the edge boundary conditions. Shear and compression loads were applied at the outboard edge using an interpolation element (Nastran RBE3) that would not add stiffness to the structure. Both designs used the identical carbon lamina material in their construction and used the same basic skin layups.

Table 1: Wing Panel Loads for Study

Wing Panel Load State	Value	Purpose
Shear	4,448 N (1,000 lbf.)	Assess Shear Buckling
Compression	17,792 N (4,000 lbf.)	Assess Compression Buckling
Normal Pressure	34.48 kPa (5 psi)	Assess out-of-plane strength, stiffness

Table 2: Wing Panel General Boundary Conditions

Analysis Type	Boundary Condition
Normal modes and normal pressure loading	All edges Simply supported
Buckling (shear and compression)	Combination of boundary conditions at edges to provide full buckling wave form development

2.1.1 Wing Panel Core Stiffened Design Description

Figure 8 shows the core stiffened wing panel design. The perimeter of the panel is composed of laminate only elements. The extent of the laminate only at the boundaries was established by the adjacent ribs, spar, and stringer attachment requirements. The interior has a laminate outer skin, core, and a thin laminate on the interior covering the core. The PMI closed cell foam core is modeled with at least two elements through the thickness to avoid node locking.

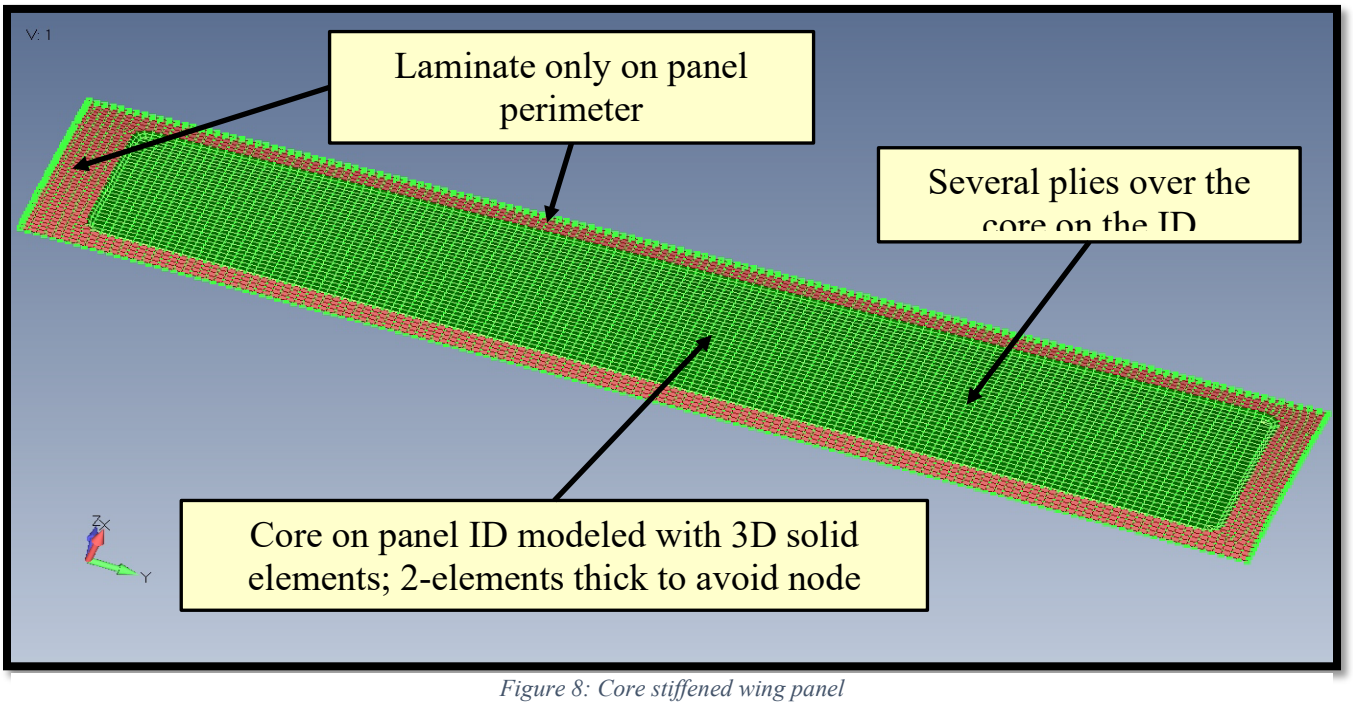

Figure 8: Core stiffened wing panel

2.1.2 **Wing Panel Stringer Stiffened Design Description**

Figure 9 describes the stringer stiffened wing panel design. It includes five chordwise stringers and two longitudinal stringers. The analysis layups follow the typical Radius stringer methodology used on other aircraft structures for blade and flange construction. Four plies are used to form the base each side of the blade and meet to form an 8-ply blade (a basic "T" construction). A triangular filler, or "noodle", is used at the intersection of the skin and blade base to help form the 90° transition. The noodle is simulated in the finite element model at the stringer blade-base intersection using CBAR elements. An element overlay technique was used when attaching the stiffener base elements to the skin. The stringer base elements were offset from the skin to properly locate them in space. Stringer spacing and blade heights were sized as the analyses dictated. Several design iterations were required to complete the dimensional sizing.

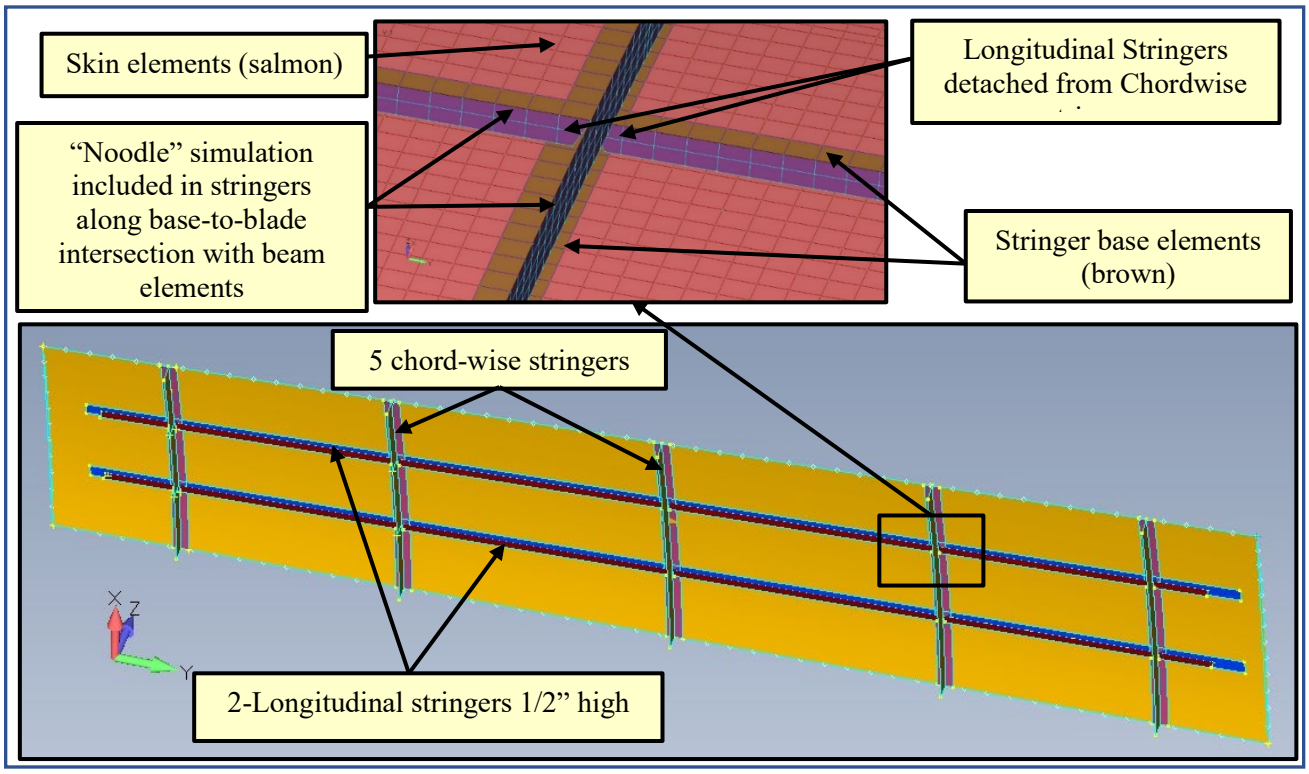

Figure 9: Stringer stiffened wing panel typical of Radius aircraft structures manufacturing methodology

2.2 Wing Spar Design Concepts

An entire wing spar was modeled using a core stiffened design and an intercostal stiffened design. As with the wing panel designs, the resulting analyses were intended as a one-to-one comparison only and not intended to represent a final design. Both spar designs generally use the same baseline flange and web layups. The intercostal design added a few local layup alterations which are discussed in Section 2.2.2. Both designs use aluminum bathtub fittings at the motor mounts and main spar-fuselage intersection to distribute the loads and boundary conditions more realistically and uniformly into the spar structures.

Figure 10 shows a schematic of the full wing spar used in the study. The figure shows six outboard motor mounts at metallic bathtub fittings, where the loads are applied. A typical aircraft weight for e-VTOL aircraft is 26,690 N (6,000 lbs.) [2]. This resulted in a load of 4,448 N (1,000 lbs.) being applied at each motor mount.

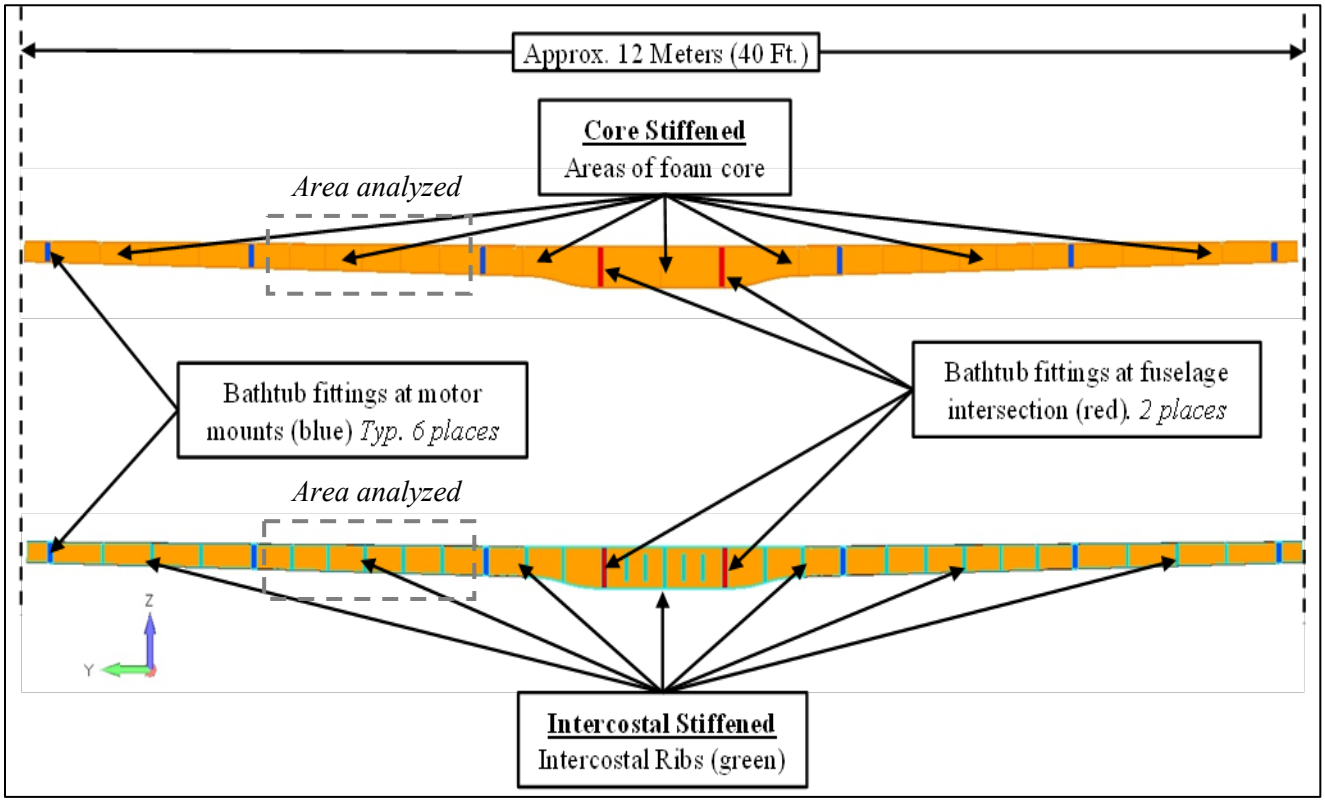

Figure 10: Core stiffened spar (top image) vs. Intercostal Rib Stiffened Spar (bottom image)

Figure 11 shows a detailed section of the spar and associated boundary outboard of the spar-fuselage intersection. This detailed section is situated between two of the motor mounts. Local coordinates were set up to correctly restrain the spar in appropriate directions. The constraint at the spar-fuselage intersection allowed rotation about the X-axis each side of the fuselage where the spar passed through but was restrained from motion in the other five axes (the X-axis is pointing out of the plane in Figure 11). The static load and normal modes analyses used the same boundary condition which restrained web out-of-plane normal motion at the boundaries simulating the restraining effect of the upper and lower wing skins. An additional restraint was added for buckling which included restraint of flange edge rotation also simulating the effect of the overlapping wing skins.

The two motor mounts shown in Figure 11show the 4,448 N load being distributed to the bathtub fittings by using an RBE3 element. The Nastran RBE3 interpolation element was used to do this as it does not impart any added stiffness to the structure.

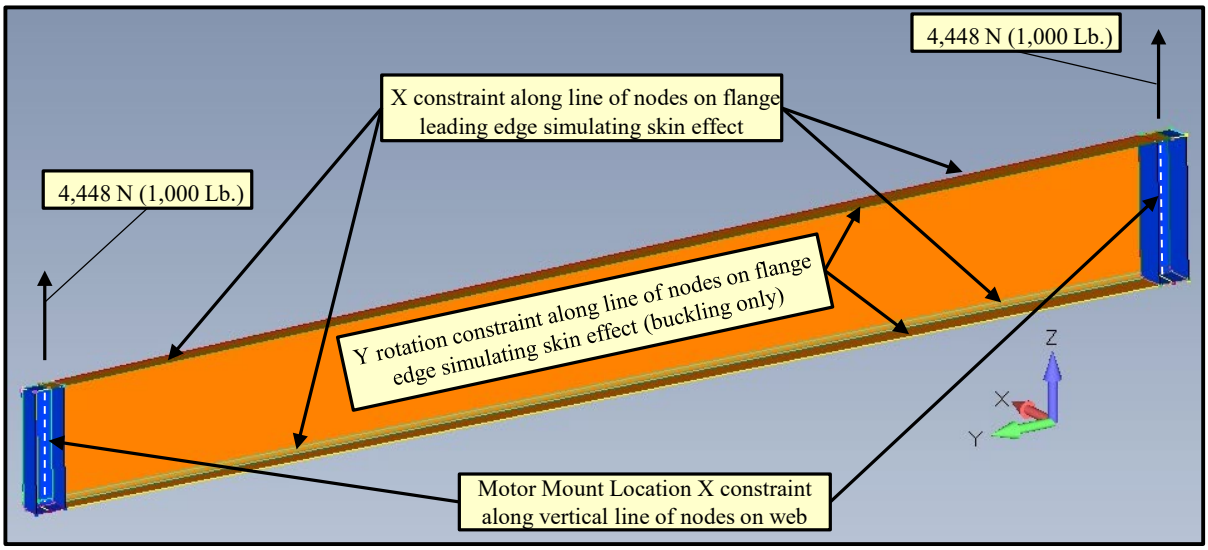

Figure 11: Basic wing spar segment and boundary condition description

2.2.1 Wing Spar Core Stiffened Design Description

Figure 12 shows the spar segment of the core stiffened design. As with the wing panel, the spar model used a combination of composite laminate shell elements and core 3D solid elements. Nastran CQUADR elements were used for the shell elements in conjunction with the ply-by-ply PCOMP material input. Nastran CHEXA and CPENTA elements were used to model the core. The perimeter of the panel is composed of laminate only elements. The extent of the laminate only at the boundaries was established by the adjacent motor mount attachment requirements. The spar web section that uses core has a thicker laminate skin on the +X side, core, and a thinner laminate skin on the -X side covering the core.

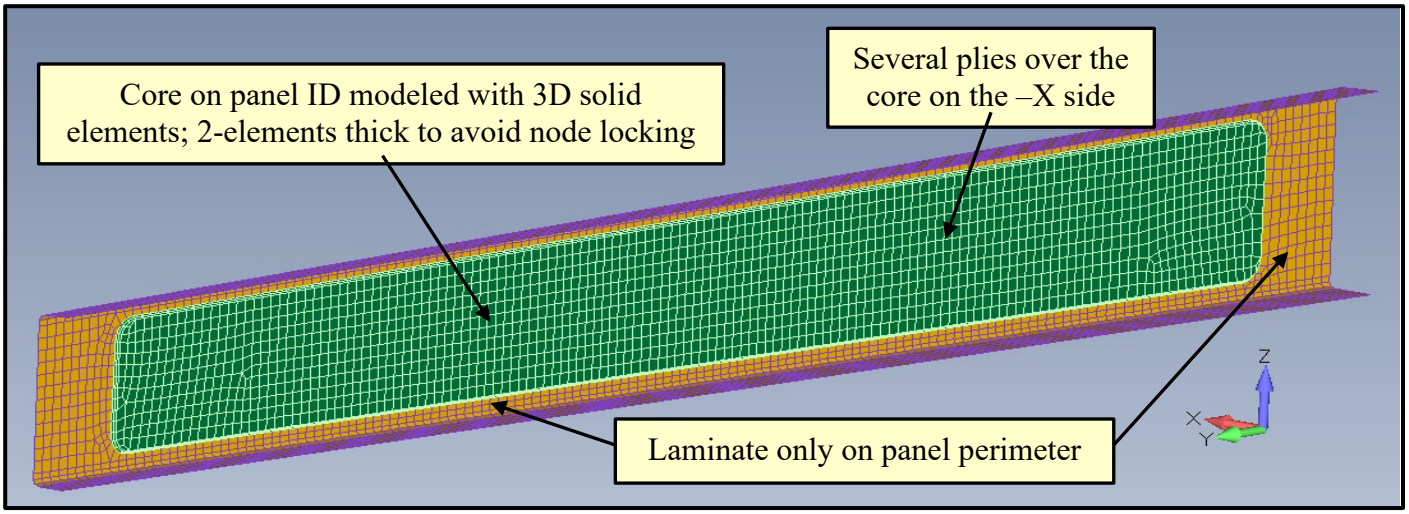

Figure 12: Core stiffened spar segment representing how the full spar was designed

2.2.2 Wing Spar Intercostal Stiffened Design Description

Figure 13 shows the spar segment of the intercostal stiffened design. The spar segment shown here has five intercostals. Intercostal spacing was varied from fuselage to wingtip. Intercostal spacing near the fuselage had a length-to-height spacing ratio of 1.3 and increased to 2.5 at the spar tip. The section shown in Figure 13 has an average intercostal spacing ratio of 1.6. The intercostal spacing was sized as dictated by the analyses results. Several design iterations were required to complete the spacing. Intercostal blade height followed the existing flange depth. The outboard spar intercostals are partials in that they terminate in the web and do not attach to the caps. The inboard intercostals as shown in Figure 13 extend and attach to the upper and lower flanges to aid in strength and buckling.

The intercostal layups are similar to how the wing panel stringers were formed. Four plies were used to form the base each side of the intercostal blade and meet to form an 8-ply blade (a basic "T" construction). A noodle was used at the intersection of the skin and blade base to help form the 90° transition. An element overlay technique was used when attaching the intercostal base elements to the web and flanges. The stringer base elements were offset from the skin to properly locate them in space.

The layup of the intercostal stiffened spar was identical to the core stiffened structure with the following exceptions. The web added a couple of 0° and 45° plies for buckling. Also, the local top flange layup in the pass-through fuselage section was carried an additional 2.5 cm into the web for improved strength.

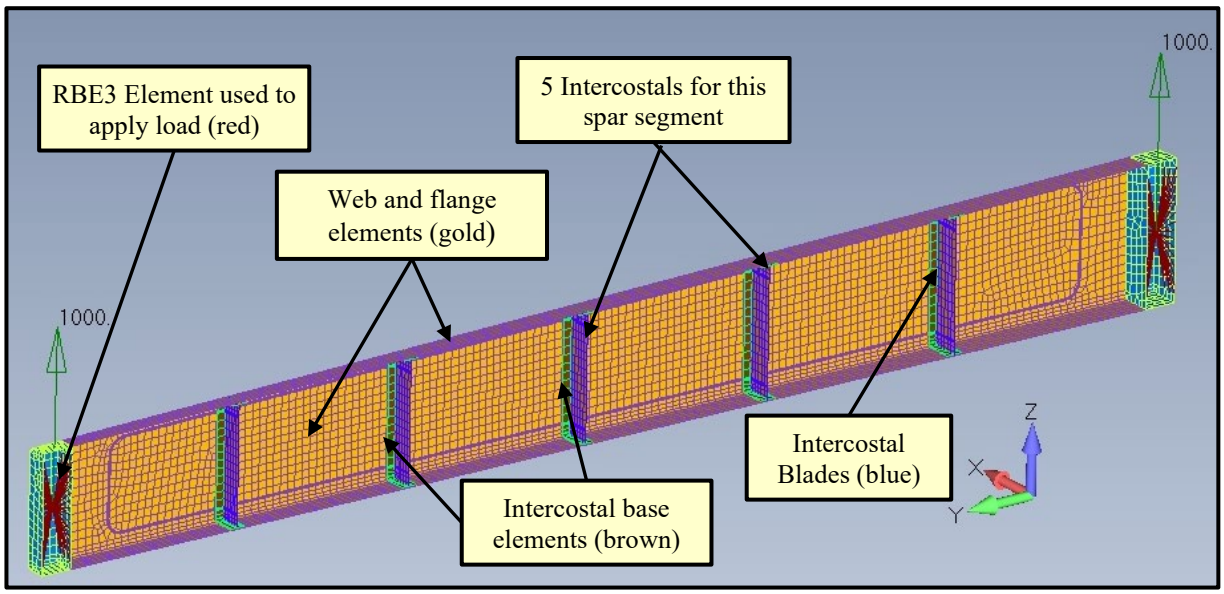

Figure 13: Intercostal stiffened spar segment representing how the full intercostal stiffened spar was designed

2.3 Manufacturing Methods

2.3.1 Manufacturing Core Stiffened Structures

Traditionally, core stiffened structures using honeycomb core on flight structures require time and labor-intensive hand layup and multiple curing and bonding steps. Newer developments with the use of rigid, closed-cell structural foam enable the production of sandwich panels with automated layup methods such as Automated Fiber Placement (AFP) and Automated Tape Laying (ATL). In 2019 foam core manufacturer Evonik, the Deutsche Zentrun fur Luft-und Raumfahrt e.V. (DLR, Stade, Germany) and the Composite Technology Centre GmbH (CTC, Stade) performed a study on a nose landing gear (NLG) door indicating that this ability to incorporate automation into the layup process as well as elimination of the two-step curing process has the potential to greatly reduce cycle times when compared to honeycomb [6]. Although the raw material costs for foam core is higher than the honeycomb core itself, a reduction in machining and core preparation costs can provide a net cost reduction for the foam core design when compare with honeycomb [7]. Additionally, the ability to use OOA processes, can reduce the cure cycle time by several hours when compared to autoclave cures. Figure 15 shows a comparison of material and Figure 14 machining costs and the results of the time study from the CTC study.

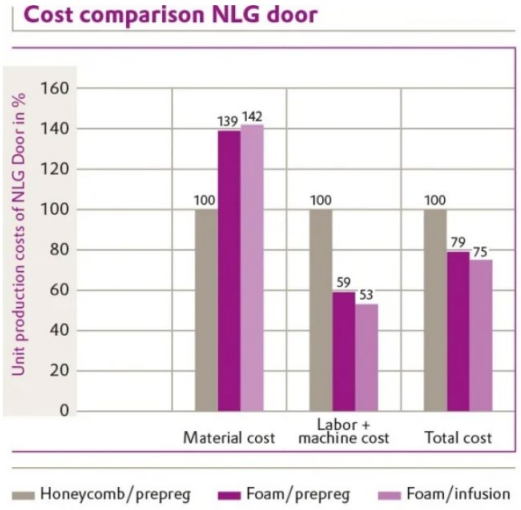

Figure 15: Cost Comparison of Honeycomb vs. Foam Core NLG Designs [7]

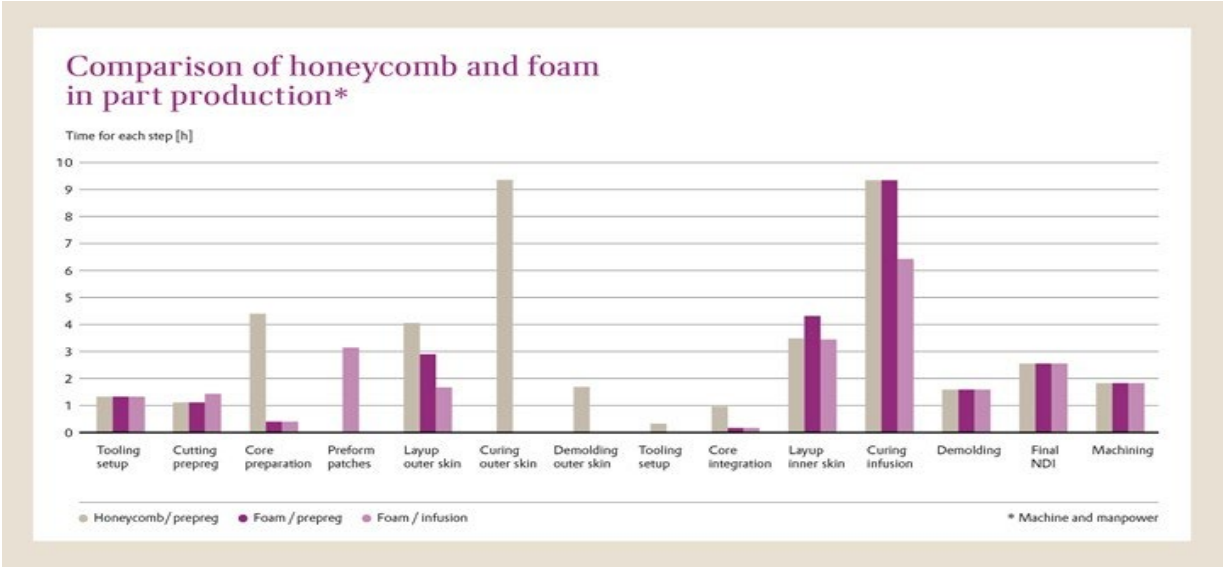

Figure 14: Study of Landing Gear Door with Closed Cell Foam vs. Honeycomb Core [6]

2.3.2 Manufacturing Stringer / Rib Stiffened Structures

Traditionally, Stringer and Rib stiffened (monolithic) structures have been produced in the autoclave with carbon fiber prepreg. More recently, developments with out-of-autoclave (OOA) processes such as Resin Transfer Molding (RTM) and Same Qualified Resin Transfer molding (SQRTM) have enabled more complex and highly integrated structures to be produced in closed molds. These closed mold OOA processes improve the process control of laminate thickness, profile dimensions, laminate quality and first pass yield, while also enabling higher levels of automation [3]. The stringer stiffened wing panel and the rib stiffened spar were assumed to be produced with the SQRTM process for the purposes of this analysis. The SQRTM process utilizes the "Same Qualified" prepregs with existing allowable databases to accelerate the FAA certification process. With RTM the preform is infused with resin and the mold is pressurized using a mold clamping system and a resin injection system. With SQRTM, however, the preform is made of prepreg (no infusion required), but the mold is still pressurized with the Same Qualified neat prepreg resin using the same mold clamping system and resin injection system that is used with RTM. The ability to control part tolerances in a closed mold and control the laminate resin pressure during the cure cycle is critical to repeatably achieving high quality composite structures with both RTM and SQRTM. The manufacturing cycle times are relatively equal for both processes, but the utilization qualified prepreg with SQRTM provides an advantage for expediting the FAA certification process.

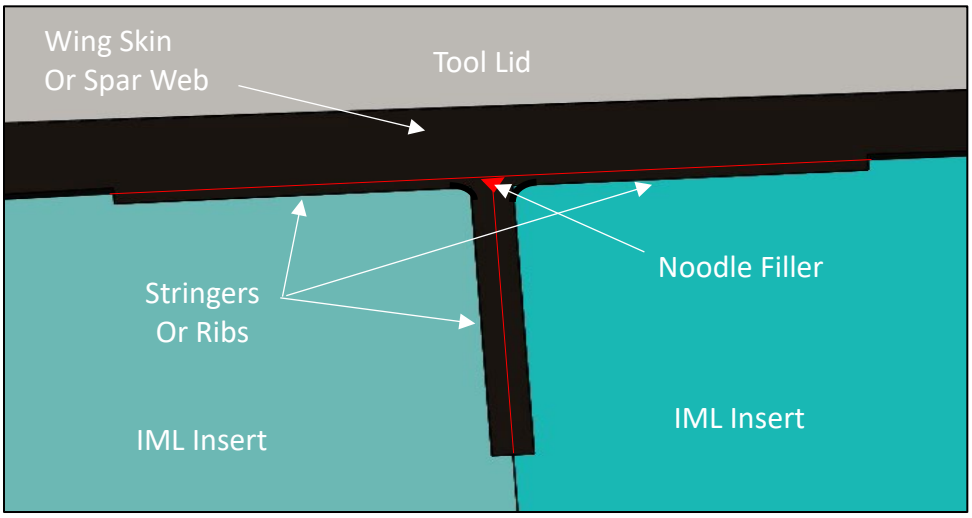

Figure 18: Stringer / Rib Cross Section in SQRTM Tooling

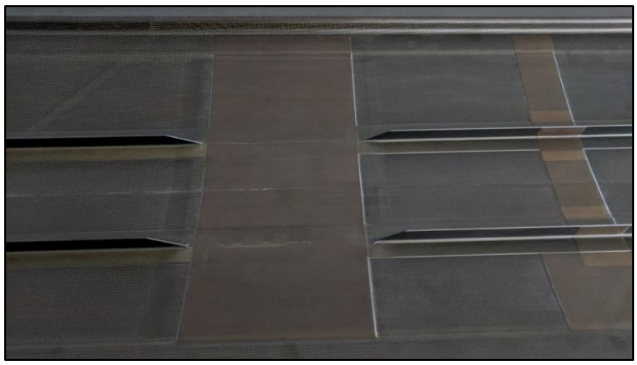

Figure 17: Stringer Stiffened Skin Example

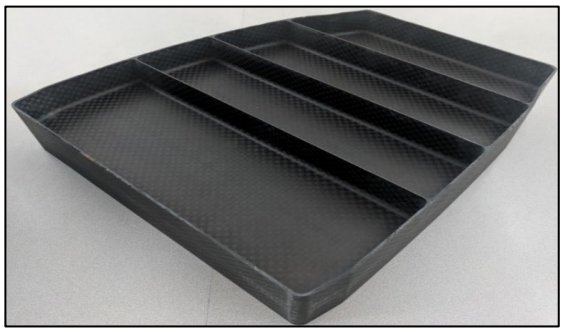

Figure 16: Intercostal Rib Stiffened Example

3. RESULTS

3.1 Design Analysis

A comparison of the analysis results comparing the two design approaches is presented. As will be shown below, the general conclusion from the analyses is that the two design approaches provide similar results.

3.1.1 Wing Skin Comparative Analysis Results

Table 3 provides a comparison of results for the core stiffened versus rib/stringer stiffened wing panel design. The table shows that for panels having similar weights, the panels had comparable shear buckling capabilities. Both designs had good compression buckling capability with the rib/stringer design being 24% higher compression capability than the core stiffened design. The wing panel stresses were compared when subjected to skin normal pressure of 34.5 kPa (5psi). The Tsai-Hill failure index (FI) was used for the stress comparison. The goal is to have the Tsai-Hill failure index below 1 when designing composites. The table shows that both designs are well below 1 with the core stiffened design being 19% less than the rib/stringer stiffened design. The maximum panel deflections with a skin normal pressure of 34.5 kPa (5psi) showed the rib/stringer design to have 28% lower panel deflection than the core stiffened design. The first normal mode for the core stiffened panel was 230 Hz while the rib/stringer stiffened panel had a mode 1 frequency of 269 Hz. The mode shapes were different due to the different stiffness reinforcing methods. The conclusion from the wing panel study is that the two panel stiffening approaches provide similar performance results with the rib/stringer design producing 28% lower panel deflection.

Table 3: Wing Panel Design Comparison

Metric	units	Core Stiffened	Rib / Stringer Stiffened	Comments
FEA Model Panel Weights	N (Lbf.)	35.8 (8.04)	35.1 (7.9)	Panel weights are similar
Shear Buckling Eigenvalue	------	1.34	1.32	Mode 1 Eigenvalue with 1,000 lbf Panel Shear Load (goal >1)
Compression Buckling Eigenvalue	------	1.48	1.83	Mode 1 Eigenvalue with 4,000 lbf Panel Compression Load (goal >1)
Tsai-Hill Failure Index (FI) 34.48 kPa (5psi) Normal Pressure	------	0.035	0.043	Rib & Stringer: local 1-element peak in stringer Core Stiffened: Uniform peak along core edge (goal >1)
Max Deflection, 34.48 kPa (5psi) Normal Pressure	mm (in.)	3.35 (0.132)	2.41 (0.095)	Rib & Stringer design: 28% lower deflection
First Vibration Normal Mode 1 (no load)	Hz.	230	269	Normal Mode 1 similar in value but different mode shapes

3.1.2 Wing Spar Comparative Analysis Results

The main spar design comparisons are listed in Table 4. The weights are similar with the intercostal stiffened design being 3% higher in weight than the core stiffened design. Eigenvalue buckling was checked with the main spar loaded at the motor mount pylons using 4,448N (1,000 lbf) load per pylon. The summed total load was 26,690 N (6,000 lbf). The resulting Eigenvalue buckling value was 1.12 and 1.17 for the core stiffened and intercostal stiffened designs respectively. The goal is to have the Eigenvalue buckling term >1. The Tsai-Hill failure index (FI) was again used for the stress comparison with the main spar loaded to 26,690 N (6,000 lbf) total load. Both designs exhibited highly local stress "hot spots" that would need to be addressed in a final design. However, the Tsai-Hill failure index shows the core stiffened design local peak stresses to be higher than the intercostal stiffened design peak stresses. Since the goal is to have the Tsai-Hill failure index below 1, both designs would need to implement local design changes to mitigate these local stresses. The main spar tip deflection shows the core stiffened design to have 17% higher tip deflection. The first normal mode for both designs is at about 22 Hz with both designs showing the same mode shape. The conclusion from the main spar study is that for similar weight designs, core stiffened and intercostal stiffened structures provide similar performance.

Table 4: Main Spar Design Comparison

Metric	units	Core Stiffened	Rib / Stringer Stiffened	Comments
Weight	N (Lbs.)	116.1 (26. 1)	119.7 (26.9)	Weights are similar
Eigenvalue Buckling (Webs)	------	1.12	1.17	Applied 6,000 lbf at engine pylons. (want eigenvalue >1)
Tsai-Hill Failure Index (FI) with full spar load	------	2.67	2.16	Some local peaks in all models (want FI<1)
Max tip Deflection	cm (in.)	45.2 (17.8)	38.5 (15.1)	At spar tip
First Vibration Normal Mode 1 (no load)	Hz	21.8	22.1	Vertical Flapping Mode

3.2 Manufacturing Approaches

The two manufacturing approaches described in section 2.3 have trade-offs regarding initial capital investment required for tooling and equipment as well as longer-term recurring costs associated with each process. By comparing factors that will drive manufacturing costs it is possible to identify the approach with the highest probability of success. Table 5 defines the factors that were selected as major decision criteria and provides a qualitative comparison.

Table 5: Evaluation Factors for Selecting a Preferred Manufacturing Approach

	Foam Core Stiffened Structures	***Skin Stiffened Structures***
Molds /Tooling & Fixtures	Single sided tooling, when viewed in isolation is simpler and lower cost than SQRTM tooling. However, it is not capable of producing highly integrated structures and the dimensions are only controlled on one surface of the structure. Additional costs will occur for tooling and fixtures required to achieve the finished assembly.	Closed mold tooling is typically more expensive than single sided tooling for an individual component. However, it capable of producing highly integrated structures with dimensional control on all surfaces of the structure. This reduces the number of ancillary tools and fixtures required to achieve the finished assembly. Final tooling and assembly costs are typically less than for single sided tooling and necessary assembly fixtures.
Equipment	Autoclaves are a large capital expense that also require significant facility upgrades for installation. Ovens are less expensive, but do not typically produce the desired laminate quality for high performance structures. The foam core requires additional machining prior to layup that is not required for rib and stringer designs.	The workcell (clamping system, mold temperature control systems and injection systems) is a large capital expense. The heating system requires some facility upgrades for high voltage, high amperage circuits, but standard factory floors do not need any modification.
Cycle Times and Labor	The inclusion of the foam core can reduce the number of prepreg plies that need to be placed and therefore shorten the layup cycle times compared to monolithic structures. However, the foam also makes some aspects of automation more difficult to implement. Autoclave and oven cure cycles are commonly in the range of 9 hours with common aerospace prepregs. Additional manufacturing bottlenecks typically result from batch processing in ovens and autoclaves.	Monolithic structures require more plies to be placed during the layup process, typically increasing the layup time when compared with foam cored structures. However, the use of existing automated layup and forming methods can minimize cycle time increases and reduce labor costs. SQRTM cure cycles are in the range of 5-6 hours with common aerospace prepregs. Small batch processing or single-piece flow in the molding process maximizes utilization rates for capital equipment.
Consumables	Autoclaves require large nitrogen purge systems, and the disposable bagging materials add to consumable costs.	The SQRTM tooling eliminates the need for vacuum bagging materials and heated platens control the temperature with minimal consumable costs. The injection resin adds costs, but since the part is not infused, the volume of resin is quite small relative to the part size.

	Foam Core Stiffened Structures	***Skin Stiffened Structures***
Cost of Quality	Singled sided tooling does not control part thickness. The part geometry and integrated features needs to remain simple, or the production yield will likely be reduced by out of tolerance dimensions. This design limitation may be a hinderance to future innovations. Additionally, foam core laminates cannot be processed at the 7-8 bar pressures used for aerospace prepregs. As a result, laminate fiber volume is lower and void content typically higher. Large batch processing in an autoclave or oven presents numerous challenges for process control on individual parts in the batch. The consumable bagging materials and the methods for installing them can be difficult to perfect at high production rates, resulting in more common vacuum leaks and poor laminate quality.	The closed mold process delivers precise tolerances with metal tooling that closes to hard stops. Part geometry can be better optimized for performance and manufacturing efficiency with higher quality. SQRTM cure cycles for wing skins and spars typically include a single, though often complex, part per cure cycle. Hydrostatic resin pressure and cure temperature profile are controlled directly for each individual part. Laminate quality is highly repeatable. Any variation in the process can be traced to the source and resolved more quickly with this approach.
Energy Consumption	The cure cycle in an autoclave or oven is typically sized based on the overall volume to be heated. Convective heating of cure batches is less efficient than other means of transferring thermal energy to the composite structures. Power consumption is increased by large fan motors to circulate the air / nitrogen in an oven or autoclave large enough for 12-meter-long structures.	The SQRTM cure cycle typically utilizes heated platens to conductively heat the mold, eliminating the energy losses in an autoclave due to heating and circulating nitrogen. The heating systems are based on the watts per sq. inch required to achieve the desired heating rate. The process can utilize aluminum molds to further reduce energy consumption.
Automation	The development of automated layup methods (ATL/AFP) will help to reduce labor costs and cycle times. AFP over 3-dimensinal geometries on foam core presents technical challenges that will be a barrier to implementation in production systems for the near term. Installing bagging materials and preparing autoclave batches typically require many manual actions that are not easily automated. Autoclaves and ovens can be provided with automated control systems to monitor and control the cure cycle.	The development of automated layup methods (ATL/AFP) will help to reduce labor costs and cycle times. Skins, c-spars, L-flange preforms and noodles all have proven methods for automated layup, forming and debulking. Automated systems to assemble and load SQRTM tooling into the SQRTM workcell for the composite cure cycle have been demonstrated. The SQRTM workcell is provided with automated control systems to monitor and control the cure cycle.

4. CONCLUSIONS

AAM vehicle flight structures can be effectively designed with both rigid, closed-cell structural foam and skin-stringer approaches. Foam core stiffened structures provide improvements over honeycomb core designs, and skin-stringer structures can provide benefits over foam core stiffened structures. The design study produced equivalent weights with improved stiffness for the skin stringer designs. The evaluation of manufacturing approaches indicates that the skin-stringer approach has the potential to deliver better quality with lower recurring costs and higher levels of automation. The SQRTM process provides reduced cycle times with out-of-autoclave production, using qualified prepreg materials for a shorter path FAA certification, while also setting the stage for further improvement with RTM resins that will be qualified in the future.

This study focused on the comparison of relatively equivalent designs. However, other significant benefits likely exist from design concepts that move beyond what is possible with core stiffened structures. Future studies, focusing on skin-stringer design concepts that increase the level of structural integration, should be considered to determine what additional weight reduction and manufacturing efficiencies can be achieved for AAM vehicles.

5. REFERENCES

1. SMG Consulting, https://aamrealityindex.com/ , June 5th, 2022.
2. Christopher B. Courtin, Ara Mahseredjian, Annick J. Dewald, Mark Drela,R. John Hansman, A Performance Comparison of eSTOL and eVTOL Aircraft. Report No. ICAT-2021-02, August 2021
3. D. Guening and F. Mathieu, Evolution in Composite Injection Moulding Processes for Wing Control Surfaces. SAMPE Journal, January / February 2016 Vol. 52, No. 1
4. Bruno Castanie, Christophe Bouvet, Malo Ginot, Review of composite sandwich structure in aeronautic applications, Composites Part C: Open Access 1 (2020)
5. Martin Meindlhumer, Konstantin Horejsi, Martin Schagerl, Manufacturing and Costs of Current Sandwich and Future Monolithic Designs of Spoilers. Journal of Aircraft, Vol. 56, No. 1, January–February 2019
6. Hannah Mason, Combination of automation, rigid foam core enable high-volume aircraft part production. Composites World, April 28, 2020.
7. Evonik Industries AG, Evonik Rohacell HERO Foam Core Used in Manufacture of Aircraft Nose Landing Gear Doors. https://www.axom.com/article.aspx?ArticleID=11463, October 16, 2014.